A Short Survey of Lens Spaces

M. Watkins

1989-90

ABSTRACT

This paper deals with a class of manifolds known as lens spaces. The majority of the work is devoted to 3-dimensional lens spaces, their properties, representations, and relationships with various areas of topology. The remainder outlines special cases.

TABLE OF CONTENTS

0. INTRODUCTION

The study of lens spaces dates back to 1908, when Tieze published his paper "Uber die topologischen invarienten mehrdimensionaler mannigfaltigkeiten", although the term "linsenraume" (lens space) was not introduced until 1930, by Seifert and Threlfall. Since then, the spaces have appeared frequently in works concerning 3-manifolds, surgery, and knot theory, and have the important distinction of being the first nontrivial collection of 3-manifolds to be entirely classified up to homeomorphism ([18]). They played an important rôle in the construction of the Poincaré Homology Sphere, and also entered into Milnor's counterexample to the Hauptvermutung. Rarely studied in their own right, they have generally been used as examples and counterexamples in the study of homology theory, Whitehead torsion, K-theory, etc. Also, there appears to have been considerable interest in the immersion and embedding properties of lens spaces in Japan during the late 1960's and 1970's (see the many references in [13]).

Because of the diverse nature of their applicability, at least five more or less distinct definitions / descriptions of the 3-dimensional lens space $L(p,q)$ can be found in modern topology texts, the definition used depending on the context in which they appear. This paper aims to reconcile the seemingly disparate models of $L(p,q)$ (section 1), collect the major results concerning the spaces (section 2), and briefly describe some of the related spaces which appear in conjunction with their study (section 3). Some areas of the theory are not very well documented in the available literature, and I have attempted to fill in any gaps that I found. This is particularly the case in 1.2.3, 1.3.10, 1.5, and 2.3.

All concepts used in this paper should be familiar to anyone whose background includes an undergraduate topology course or equivalent. However, little space is devoted to examples, so some additional reading may be required in some areas.

1. MODELS OF THE 3-DIMENSIONAL LENS SPACE $L(p,q)$

Five models of the lens space $L(p,q)$ and demonstrations of their equivalences follow. Throughout, it is assumed that $\gcd(p,q)=1$ and $0 \leq q < p$, although the range of indices can be extended in some cases. A full treatment of this matter is given in 3.2.

1.1 The first model of $L(p,q)$ is formulated in purely algebraic terms and is used to define the space in [1], [3], [4], [11], [19], and [22]. First, some preliminary definitions and results are needed. These conform to the notation and terminology of [1], [11], and to a lesser extent, [4].

1.1.1 A group G <u>acts on</u> a set X if there is a map $F: G \times X \to X$ where, if we denote $f(g,x)$ by $g \cdot x$,

(1) $1 \cdot x = x \quad \forall x \in X$ (where 1 is the identity in G)

(2) $g \cdot (h \cdot x) = (gh) \cdot x \quad \forall g,h \in G$ and $\forall x \in X$

1.1.2 If G acts on a topological space X, and for each $g \in G$, the mapping $\theta_g : X \to X$ given by $\theta_g(x) = g \cdot x$ is a homeomorphism, we say X is a <u>G-space</u>.

1.1.3 If X is a G-space such that $g \cdot x = x$ for some $x \Rightarrow g = 1$, then we say G <u>acts freely</u> on X.

1.1.4 If G acts on X, X/G denotes the set of equivalence classes $\{[x] : x \in X\}$ where $[x_1] = [x_2] \Leftrightarrow x_1 = g \cdot x_2$ for some $g \in G$. X/G is called the <u>orbit space</u> of X over G, and the $G \cdot x$ constitute a collection of disjoint <u>orbits</u>, corresponding to the equivalence classes.

1.1.5 An <u>n-manifold</u> M is a Hausdorff space such that each point in M has a neighbourhood homeomorphic to $\mathring{D}^n = \{x \in \mathbb{R}^n : \|x\| < 1\}$ (equivalently, each point in M has a neighbourhood homeomorphic to $\mathbb{R}^n$, as $\mathring{D}^n \cong \mathbb{R}^n$, given by $h: \mathring{D}^n \to \mathbb{R}^n$ where $h(x) = \frac{x}{1-\|x\|}$).
An <u>n-manifold-with-boundary</u> M is a Hausdorff space such that each point in M has a neighbourhood homeomorphic to either $\mathbb{R}^n$ or the upper half-space $\mathbb{R}^n_+ = \{x = (x_1, \ldots, x_n) \in \mathbb{R} : x_n \geq 0\}$. The set of points in M having the latter but not the former can be shown to be an $(n-1)$-manifold ([11] p.91) which is called the <u>boundary</u> of M, denoted ∂M.

1.1.6 The following lemma is obtained by combining two results from [11] (p. 54-55).
<u>Lemma</u>: If X is a compact Hausdorff G-space with G finite, then X/G is compact Hausdorff.
<u>Proof</u>: Let $p: X \to X/G$ be given by $p(x) = [x]$. If we treat X/G as a quotient space, then open sets in X/G are defined in terms of their p-preimage sets in X, and p is automatically continuous. X/G is the continuous image of a compact space X and is therefore compact by elementary topology. Suppose $[x_1], [x_2] \in X/G$ and $[x_1] \neq [x_2]$. This means $g_1 \cdot x_1 \neq g_2 \cdot x_2$ for all $g_1, g_2 \in G$, so $p^{-1}([x_1]) = \{g \cdot x_1 : g \in G\}$ and $p^{-1}([x_2]) = \{g \cdot x_2 : g \in G\}$ are disjoint subsets of X. Since they are finite sets, repeated application of the Hausdorff property can be used to construct disjoint U_1, U_2 open in X with $p^{-1}([x_1]) \subseteq U_1$ and $p^{-1}([x_2]) \subseteq U_2$ (as in [11]). Now $p^{-1}(p(X \setminus U_i)) = \bigcup_{g \in G} g \cdot (X \setminus U_i) = \bigcup_{g \in G} \theta_g(X \setminus U_i)$, so $p^{-1}(p(X \setminus U_i))$ is the union of finitely many closed sets, for $i = 1,2$, (the θ_g are all homeomorphisms) and consequently closed in X. So $p(X \setminus U_i)$ is closed in X/G and $W_i = (X/G) \setminus p(X \setminus U_i)$ is open in X/G, for $i = 1,2$.
We have $p^{-1}([x_i]) \subseteq U_i \Rightarrow [x_i] \notin p(X \setminus U_i) \Rightarrow [x_i] \in W_i$ for $i = 1,2$.
Further, $W_1 \cap W_2 = ((X/G) \setminus p(X \setminus U_1)) \cap ((X/G) \setminus p(X \setminus U_2)) = (X/G) \setminus (p(X \setminus U_1) \cup p(X \setminus U_2)) = (X/G) \setminus p((X \setminus U_1) \cup (X \setminus U_2))$
$= (X/G) \setminus p(X \setminus (U_1 \cap U_2)) = (X/G) \setminus p(X) = \phi$. So the Hausdorff condition is satisfied on X/G.

1.1.7 The proof of the following theorem is required as one of the more difficult exercises in [11].
<u>Theorem</u>: If G is a finite group acting freely on a G-space X, and X is a compact n-manifold, then X/G is a compact n-manifold.
<u>Proof</u>: Because X is an n-manifold, it is Hausdorff, and the conditions of 1.1.6 are satisfied. So X/G is compact Hausdorff, and it only remains to be seen that each point in X/G has a neighbourhood homeomorphic to $\mathbb{R}^n$. Let $G = \{1 = g_0, g_1, \dots, g_m\}$. Given $[x] \in X/G$, we have $x \in X$ with $p(x) = [x]$. Because G acts freely, $g_m \cdot x = x \Rightarrow m = 0$, so by repeated application of the Hausdorff property, it is possible to construct open neighbourhoods $\mathcal{U}_0, \mathcal{U}_1, \dots, \mathcal{U}_m$ of $g_0 \cdot x, g_1 \cdot x, \dots, g_m \cdot x$ respectively, with $\mathcal{U}_0 \cap \mathcal{U}_i = \phi$ for $1 \le i \le m$. Then $\mathcal{U} = \bigcap_{i=0}^{m} g_i^{-1} \cdot \mathcal{U}_i = \bigcap_{i=0}^{m} \theta_{g_i^{-1}}(\mathcal{U}_i)$ is clearly an open neighbourhood of x (the $\theta_{g_i^{-1}}$ are all homeomorphisms). We know that x has some open neighbourhood W_x in X with $W_x \cong \mathbb{R}^n$ given by some $h: W_x \to \mathbb{R}^n$. $W_x \cap \mathcal{U}$ is open in W_x, so $h(W_x \cap \mathcal{U})$ is open in $\mathbb{R}^n$. Since $h(x) \in h(W_x \cap \mathcal{U})$, $\exists\, \varepsilon > 0$ with $N_\varepsilon(h(x)) \subseteq h(W_x \cap \mathcal{U})$. Then $V_x = h^{-1}(N_\varepsilon(h(x))) \cong N_\varepsilon(h(x)) \cong \mathbb{R}^n$ is an open neighbourhood of x in $\mathcal{U}$. Next we will see that the mapping $(p|V_x): V_x \to p(V_x)$ is a homeomorphism: $p|V_x$ is injective as $(p|V_x)(x_1) = (p|V_x)(x_2) \Rightarrow [x_1] = [x_2] \Rightarrow x_1 = g_k \cdot x_2$ for some $g_k \in G$. Then $x_1, x_2 \in V_x \Rightarrow x_1, x_2 \in \mathcal{U}$ $\Rightarrow x_1 \in g_0^{-1} \cdot \mathcal{U}_0 = \mathcal{U}_0$ and $x_2 \in g_k^{-1} \cdot \mathcal{U}_k \Rightarrow x_1 = g_k \cdot x_2 \in \mathcal{U}_0 \cap \mathcal{U}_k \Rightarrow \mathcal{U}_0 \cap \mathcal{U}_k \neq \phi \Rightarrow k = 0 \Rightarrow g_k = 1$ $\Rightarrow x_1 = x_2$. $p|V_x$ is surjective by definition. Since $p: X \to X/G$ is open (simple result, see [11]) and continuous, the restriction of p to an open set will also be open and continuous. So $p|V_x$ is a homeomorphism, and consequently $p(V_x) \cong V_x \cong \mathbb{R}^n$. $p(V_x)$ is the required open neighbourhood of $[x]$ in X/G, and the result follows.

1.1.8 The 3-dimensional sphere S^3 is defined to be the set $\{(z_0, z_1) \in \mathbb{C}^2 : |z_0|^2 + |z_1|^2 = 1\}$.

1.1.9 The cyclic group with p elements is $\mathbb{Z}_p = \{0, 1, \dots, p-1\}$ (p is not necessarily prime), where addition is defined mod p, and 0 is the additive identity.

1.1.10 Fix some $q \in \mathbb{Z}$ with $0 \le q < p$ and $\gcd(p,q) = 1$, and let $\mathbb{Z}_p$ act on S^3 as follows: $m \cdot (z_0, z_1) = \left(e^{\frac{2\pi i m}{p}} \cdot z_0, e^{\frac{2\pi i q m}{p}} \cdot z_1\right)$
This constitutes a group action, since:

1. $0 \cdot (z_0, z_1) = (e^0 \cdot z_0, e^0 \cdot z_1) = (z_0, z_1)$
2. $m \cdot (n \cdot (z_0, z_1)) = m \cdot \left(e^{\frac{2\pi i n}{p}} \cdot z_0, e^{\frac{2\pi i n q}{p}} \cdot z_1\right) = \left(e^{\frac{2\pi i (m+n)}{p}} \cdot z_0, e^{\frac{2\pi i (m+n) q}{p}} \cdot z_1\right) = (m+n) \cdot (z_0, z_1)$

and the action is well-defined since $m_1 \equiv m_2 \pmod p \Rightarrow e^{\frac{2\pi i m_1}{p}} = e^{\frac{2\pi i m_2}{p}} \Rightarrow m_1 \cdot (z_0, z_1) = m_2 \cdot (z_0, z_1)$.

Let $\theta_m : S^3 \to S^3$ be defined by $\theta_m(z_0, z_1) = m \cdot (z_0, z_1) = \left(e^{\frac{2\pi i m}{p}} \cdot z_0, e^{\frac{2\pi i m q}{p}} \cdot z_1\right)$. By well-known results concerning product spaces and mappings, θ_m can be seen to be continuous and to have a continuous inverse for each m. Each θ_m is also clearly bijective, and therefore a homeomorphism. S^3 is consequently a $\mathbb{Z}_p$-space.

$\mathbb{Z}_p$ acts freely on S^3 since $m \cdot (z_0, z_1) = (z_0, z_1) \Rightarrow e^{\frac{2\pi i m}{p}} \cdot z_0 = z_0$ and $e^{\frac{2\pi i m q}{p}} \cdot z_1 = z_1$, the first equation allowing two possible cases: $e^{\frac{2\pi i m}{p}} = 1$ or $z_0 = 0$.

Case 1: $e^{\frac{2\pi i m}{p}} = 1 \Rightarrow m/p \in \mathbb{Z} \Rightarrow p \mid m \Rightarrow m = 0$ in $\mathbb{Z}_p$

Case 2: $z_0 = 0 \Rightarrow |z_1| = 1 \Rightarrow z_1 \neq 0 \Rightarrow e^{\frac{2\pi i m q}{p}} = 1 \Rightarrow \frac{mq}{p} \in \mathbb{Z} \Rightarrow p \mid mq \Rightarrow p \mid m$ (as $\gcd(p,q) = 1$)
$\Rightarrow m = 0$ in $\mathbb{Z}_p$

1.1.11 We now define $L(p,q)$ to be the orbit space $S^3/\mathbb{Z}_p$ with respect to this action.

Consider the definition of S^3 given in 1.1.8. If we set $z_0 = x_1 + ix_2$, $z_1 = x_3 + ix_4$, we see that $S^3 = \{(x_1, x_2, x_3, x_4) \in \mathbb{R}^4 : x_1^2 + x_2^2 + x_3^2 + x_4^2 = 1\}$. That is, S^3 is the unit sphere in 4-space.

By the Heine-Borel theorem S^3 is compact, since it is a closed bounded subset of $\mathbb{R}^4$. Further, a <u>stereographic projection</u> can be used to show that S^3 is a 3-manifold (see [11] p.68). We have seen that S^3 is a $\mathbb{Z}_p$-space upon which the finite group $\mathbb{Z}_p$ acts freely. Therefore, by 1.1.7, $L(p,q)$ is a compact 3-manifold.

1.2 The next model of $L(p,q)$ is of a more geometric nature. It appears in three slightly different versions, distributed more or less uniformly throughout the literature:

1.2.1 (i) (Appears in [22], [24]) The solid "lensform" shown in FIG 1 with upper and lower caps identified via an orthogonal projection after a $\frac{2\pi q}{p}$-radian positive rotation of the upper cap with respect to the lower (more details to follow)

(ii) (Appears in [14], [19], [24]) The unit ball $D^3 = \{x \in \mathbb{R}^3 : \|x\| \leq 1\}$ as shown in FIG 2 with analagous identifications to (i)

(iii) (Appears in [1], [10]) The polyhedron shown in FIG 3 which consists of two pyramids with regular p-gon bases, joined at their bases, and with upper and lower faces identified after a twist identification analagous to (i)

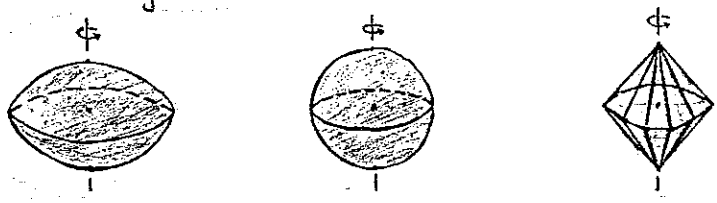

FIG1 FIG2 FIG3

Since all three solids are obviously homeomorphic with analagous identifications, the three resulting identification spaces will be homeomorphic. Version (i) turns out to be the most useful model for our purposes, so we shall hereby abandon versions (ii) and (iii).

1.2.2 A more accurate description of (i) will be required: Consider a solid lens-shaped cell whose surface consists of two identical, radially symmetric caps which meet at a circular rim. The exact proportions are unimportant. Label the north and south poles N and S respectively, and partition the circular rim into p equal arcs separated by points $x_0, \ldots, x_{p-1}$. Join each x_i to N and to S with curvilinear segments to divide each cap into p identical triangular sectors.

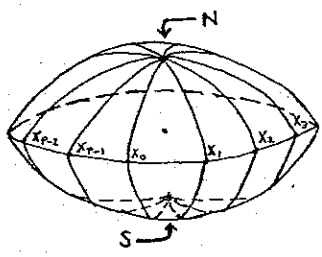

FIG4

The $\frac{2\pi q}{p}$-radian twist and projection mentioned before result in each $\Delta N x_i x_{i+1}$ being identified with $\Delta S x_{q+i} x_{q+i+1}$ (where all subscripts are taken mod p). Note that $\{x_0, x_q, x_{2q}, \ldots, x_{(p-1)q}\}$ are all identified, and since $\gcd(p,q)=1$, this is just the set $\{x_0, x_1, \ldots, x_{p-1}\}$. So all vertices are identified together, as are all equatorial arcs $\widehat{x_i x_{i+1}}$, for similar reasons. Obviously N and S are identified.

Next, we shall see that model 1.2 is equivalent to model 1.1. That is, that the identification space described above represents the orbit space $S^3/\mathbb{Z}_p$.

1.2.3 Since it is rather difficult to picture as a sphere in 4-space, the first step will be to construct an easily-visualised model of S^3.

S^3 is the set of ordered pairs of complex numbers (z_0, z_1) with $|z_0|^2+|z_1|^2=1$. If we use the modular representations $z_0=r_0e^{i\theta_0}$ and $z_1=r_1e^{i\theta_1}$, then $r_0^2+r_1^2=1$. Further, fixing r_1 fixes $r_0=(1-r_1^2)^{1/2}$. So (z_0,z_1) can be associated with a real triple (r_1,θ_0,θ_1), $0\le r_1\le 1$, $0\le\theta_0,\theta_1<2\pi$. The collection of triples suggests a solid torus in $\mathbb{R}^3$, and when suitably adapted, this will in fact become our model of S^3.

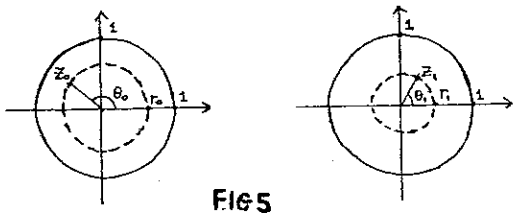

FIG 5

Note that when $r_1=0$ or 1, the one-to-one correspondence $(z_0,z_1)\leftrightarrow(r_1,\theta_0,\theta_1)$ breaks down:

1. If $r_1=0$, then $r_0=1$, and $(z_0,z_1)=(e^{i\theta_0},0)$ which is independent of θ_1. Hence we need $(0,\theta_0,\theta_1)=(0,\theta_0,\theta_1')$ for all $0\le\theta_1,\theta_1'<2\pi$
2. If $r_1=1$, then $r_0=0$, and $(z_0,z_1)=(0,e^{i\theta_1})$ which is independent of θ_0. Hence we need $(1,\theta_0,\theta_1)=(1,\theta_0',\theta_1)$ for all $0\le\theta_0,\theta_0'<2\pi$

If we represent points of a solid torus T with meridianal radius 1 as shown in FIG 6, then the first condition is automatically fulfilled, since points on the "central circle" $r_1=0$ are independent of θ_1.

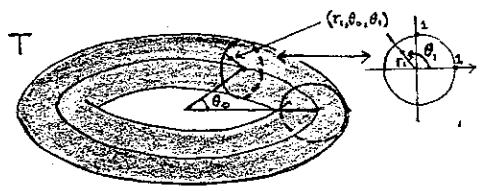

FIG 6

In order to fulfil the second condition, we must appropriately identify points on $r_1=1$, which is $\partial T = S^1\times S^1$, a torus. Examining the condition, we see that for each c, $0\le c<2\pi$, all points on $\{(r_1,\theta_0,\theta_1): \theta_1=c, r_1=1\}$, a latitude on ∂T, are to be identified together. Hence each latitude becomes a single point, and the boundary is effectively reduced to a single meridian.

Cutting T across an appropriately chosen half-plane gives the solid cylinder of FIG 7 with identified ends, and each of the suggested vertical segments identified to a single point thereon. The result is homeomorphic to a solid ball D^3 with upper and lower hemispheres identified via orthogonal projection (FIG 8). To see this, collapse the vertical segments of FIG 7 simultaneously.

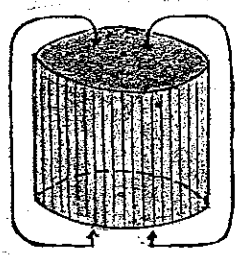

FIG 7

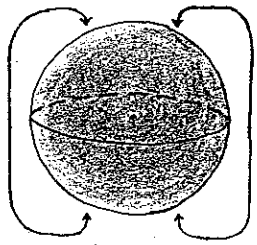

FIG 8

This is a widely used identification space in topology texts; however, I have yet to come across the above proof (or any other) demonstrating that it in fact represents S^3. Note that we could equally-well choose a lensform representation with analagous identifications. This would suggest that, provided model 1.2 is valid, $L(1,q) \cong S^3$ for all $q \in \mathbb{Z}$, a result we will later confirm. (Of course, if $q \neq 0$, $L(1,q)$ is an abuse of our convention on indices; however, in this model it has a well-defined interpretation. See 3.2).

The above demonstration will also be helpful in visualising the orbits induced by the action of $\mathbb{Z}_p$ on S^3, which we shall now calculate.

1.2.4 First, it is necessary to determine the equivalence classes of T (and hence of S^3) under the action of $\mathbb{Z}_p$ given by $m\cdot(z_0,z_1) = (z_0\cdot e^{\frac{2\pi i m}{p}}, z_1\cdot e^{\frac{2\pi i q m}{p}}) = (r_0 e^{i(\theta_0 + \frac{2\pi m}{p})}, r_1 e^{i(\theta_1 + \frac{2\pi q m}{p})})$. Using our solid torus coordinates, $m\cdot(r,\theta_0,\theta_1) = (r, \theta_0 + \frac{2\pi m}{p}, \theta_1 + \frac{2\pi q m}{p})$. Notice that the value of r is unaffected by $\mathbb{Z}_p$-action. Hence, we can restrict our attention to individual tori $r=c$ $(0 \le c \le 1)$, which will be denoted T_c. Note that $T = \bigcup_{0\le c\le 1} T_c$; also T_0 and T_1 are special cases - they will be treated later.

When $0<c<1$, T_c can be pictured as a square with identified edges, with the horizontal axis acting as the θ_1-axis and the vertical as the θ_0-axis, both ranging from 0 to 2π on the square.

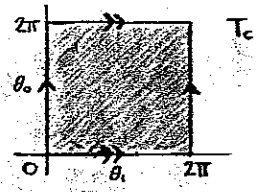

FIG 9

The action of m on the point (θ_0,θ_1) results in the point $(\theta_0 + \frac{2\pi m}{p}, \theta_1 + \frac{2\pi q m}{p})$, so all actions of $\mathbb{Z}_p$ are translations along lines with gradient $\frac{2\pi m}{p} / \frac{2\pi q m}{p} = 1/q$.
Consider as an example the case $p=5, q=3$. If a line of gradient $1/3$ is drawn through a point on T_c, we see that the equivalence class of the point contains $p=5$ points equally spaced along the line.

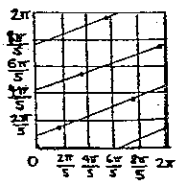

FIG 10

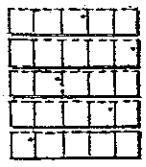

FIG 11

Note that the equivalence class contains exactly one point in each of the horizontal bands of the decomposition shown in FIG 11, and of course an analagous result will hold for any p, q with $\gcd(p,q)=1$. So a single horizontal band of width $\frac{2\pi}{p}$ contains exactly one point from each equivalence class of T_c. We can therefore define the orbit space as $T_c/\mathbb{Z}_p = \{(r,\theta_0,\theta_1) : r=c, 0\le\theta_0<\frac{2\pi}{p}, 0\le\theta_1<2\pi\}$. This is a short tube with ends "twist identified" by a $\frac{2\pi q}{p}$ twist.

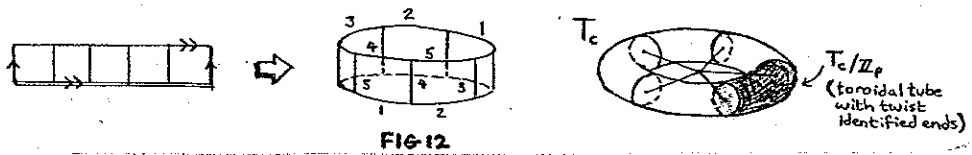

FIG 12

There are two special cases to be taken into consideration: T_0 (the central circle) and T_1 (∂T with identifications). These are degenerate tori, so the orbit spaces cannot be pictured as in FIG 12.

Case T_0: T_0 is the circle $r_1=0$. The action of m on a point of T_0 sends $\theta_0 \to \theta_0 + \frac{2\pi m}{p}$, inducing a $\frac{2\pi m}{p}$ rotation, so each equivalence class contains exactly one point in each $\frac{2\pi}{p}$ radian arc. In particular, the arc $0\le\theta_0<\frac{2\pi}{p}$ has exactly one point from each equivalence class, and $T_0/\mathbb{Z}_p$ can be viewed as an arc with identified endpoints.

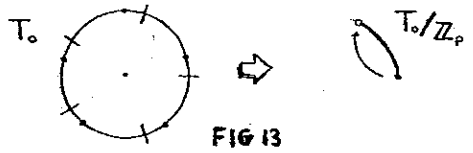

FIG 13

Case T_1: T_1 is the boundary ∂T with latitudes identified to a point each. This can be thought of as a circle S^1. The action of m on a point (latitude) of T_1 sends $\theta_1 \to \theta_1 + \frac{2\pi q m}{p}$, inducing a $\frac{2\pi q m}{p}$ rotation. Since $\gcd(p,q)=1$, if we partition S^1 into p equal arcs $0\le\theta_1<\frac{2\pi}{p}, \ldots, \frac{2(p-1)\pi}{p}\le\theta_1<2\pi$, then all of these get identified.

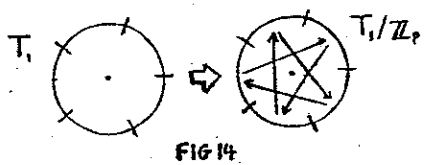

FIG 14

1.2.5 Because $\mathbb{Z}_p$-action leaves points on their respective tori T_c, it is evident that $S^3/\mathbb{Z}_p = \bigcup_{0\le c\le 1} T_c/\mathbb{Z}_p$. This is a collection of nested tubes with radii $0\le r<1$ whose ends are twist-identified by a $\frac{2\pi q}{p}$-radian twist, and a boundary of latitude-segments which are identified to single points, and then further identified from p arcs to one (FIGS 15 and 16).

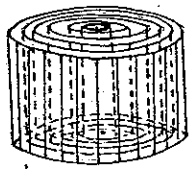

FIG 15

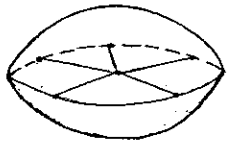

FIG 16

If we first collapse the latitude-segments to points, we get a lensform whose circular rim is divided into p equal arcs, all identified together. The upper and lower caps of the lensform correspond to the ends of the solid cylinder of FIG 15, and are therefore twist-identified by a $\frac{2\pi q}{p}$ twist. This is of course $L(p,q)$ as initially described in model 1.2, so models 1.1 and 1.2 describe the same space and are consequently equivalent.

Of all the sources I have encountered, only [1] and [19] describe $L(p,q)$ as both an orbit space <u>and</u> an identification space, and both fail to demonstrate the equivalence of these spaces.

1.3 At this point, a third model of $L(p,q)$ is introduced: $L(p,q)$ is the 3-manifold of Heegaard genus 1 whose Heegaard diagram consists of a (p,q) torus knot on the surface of a solid torus. [2], [6], [9], [16], [19], and [24] all describe $L(p,q)$ in this way.

In order to understand this description, we must first introduce some definitions and results:

1.3.1 A <u>surface</u> is a compact, connected 2-manifold.

1.3.2 A surface M is <u>orientable</u> if its 2nd Homology group $H_2(M)$ is non-trivial (see [1]).

1.3.3 The famous Classification Theorem states that every orientable surface is of the form $S^2 \# nT$ for some well defined $n \geq 0$. That is, n "handles" sewn to the 2-sphere. n is called the <u>genus</u> of the surface, and any n-genus surface will be homeomorphic to the surface depicted in FIG 17.

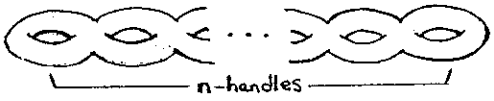

FIG 17

1.3.4 A <u>handlebody</u> is a 3-manifold-with-boundary consisting of an orientable surface and its interior. The <u>genus</u> of a handlebody H is defined to be the genus of the surface ∂H, as defined in 1.3.3.

1.3.5 A <u>Heegaard splitting</u> of a 3-manifold is its decomposition into two handlebodies H_1, H_2 of equal genus whose surfaces are identified via a homeomorphism $h: \partial H_1 \to \partial H_2$.

1.3.6 <u>The Heegaard genus</u> of a 3-manifold M is the minimal n for which M can be decomposed into two n-genus handlebodies via a Heegaard splitting.

1.3.7 Suppose M has Heegaard genus n, and that the n-genus handlebodies H_1, H_2 with surface identification $h: \partial H_1 \to \partial H_2$ constitute a Heegaard splitting of M. Then the associated <u>Heegaard diagram</u> of M is H_2 together with the disjoint simple closed curves $h(m_1), \ldots, h(m_n)$ where $m_1, \ldots, m_n$ are the canonical meridians chosen on ∂H_1 as shown in FIG 18.

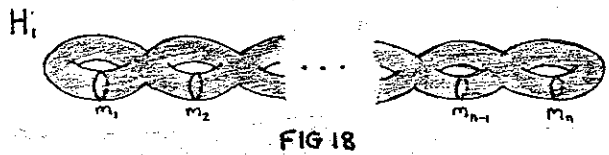

FIG 18

[24] (p. 254) contains a succinct proof that knowledge of the $h(m_i)$ on ∂H_2 alone suffices in the reconstruction of a 3-manifold homeomorphic to M. That is, if $h^*: \partial H_1 \to \partial H_2$ with $h^*(m_i) = h(m_i)$ for $1 \leq i \leq n$, then $H_1 \cup_{h^*} H_2 \cong H_1 \cup_h H_2 = M$.

1.3.8 The fundamental group of a torus can be shown to be $\mathbb{Z}^2$, the free group on two generators: If we fix a point x_0 on a torus M and denote the canonical latitude and meridian (with fixed relative orientations) passing through x_0 as ℓ, m respectively, then ℓ and m can be seen to generate $\pi_1(M, x_0)$.

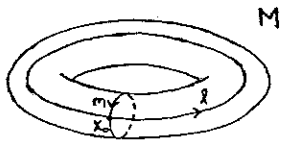

FIG 19

That is, every closed loop on M based at x_0 is in the homotopy class of some $a\ell + bm$ ($a, b \in \mathbb{Z}$, the signs of a, b representing the directions in which ℓ, m are to be traversed). If $\gcd(p,q)=1$, then a member of the loop class $[p\ell + qm]$ is called a <u>(p,q) torus knot</u>. Note that $(1,0)$ and $(0,1)$ torus knots are latitudes and meridians, respectively. For further details on torus knots, see [6], [11], or [19].

1.3.9 We are now in a position to interpret model 1.3. It describes $L(p,q)$ as the result of joining two solid tori (i.e. genus 1 handlebodies) T_1, T_2 via a homeomorphism $h: \partial T_1 \to \partial T_2$ where h takes a meridian m on ∂T_1 to a torus knot (p,q) on ∂T_2.

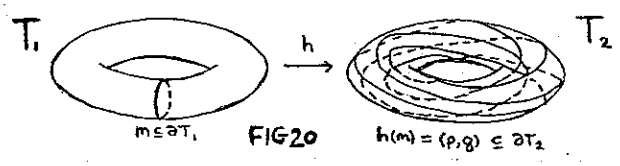

FIG 20

This illustrates the case for $(p,q) = (5,3)$, as will all further figures.

As would be expected, the 3-manifold resulting directly from this identification is difficult to visualise at first. However, we shall eventually see that it is in fact the lens space $L(p,q)$, as described by model 1.2.

1.3.10 Cutting T_2 across a suitable half-plane yields a solid cylinder with p disjoint sections of the knot (p,q) along its side. To see this, consider the identification space representing ∂T_2 as shown in FIG 21. A (p,q) torus knot can be represented as a line through o with a p/q gradient (FIG 22).

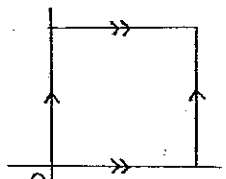

FIG 21

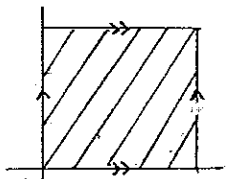

FIG 22

Cutting T_2 across a half-plane orthogonally has the effect of disconnecting the identification square horizontally. This will result in p disjoint line segments curved around the side of a solid cylinder with identified ends (FIG 23) which is equivalent to the cylinder of FIG 24 with a $\frac{2\pi q}{p}$-radian twist.

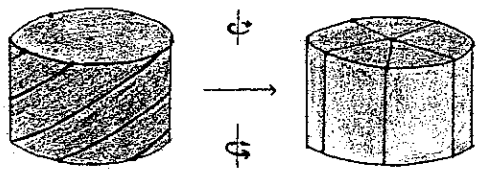

FIG 23 FIG 24

Since $(p,q)=1$, by Bezout's Identity, there exist $r, s \in \mathbb{Z}$ such that $pr + qs = 1$. Hence $qs \equiv 1 \pmod{p}$, meaning q has an inverse $s = q^{-1}$ in $\mathbb{Z}_p$. s is unique in $\mathbb{Z}_p$, as $qs' \equiv 1 \pmod{p}$ $\Rightarrow sqs' \equiv s \pmod{p} \Rightarrow s' \equiv s \pmod{p}$.

Cutting T_1 through a half-plane containing the meridian m gives a solid cylinder with identified ends and a copy of m around each end (FIG 25). Now twist the cylinder so that the ends are offset by $\frac{2\pi q^{-1}}{p}$ radians (FIG 26) and decompose the cylinder into p equal "wedges" as shown in FIG 27.

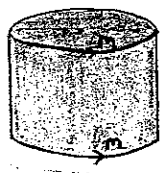

FIG 25

FIG 26

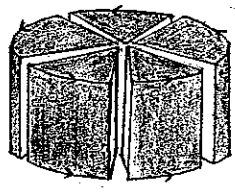

FIG 27

Because of the twist, if we label the upper wedge-faces in a positive circuit $0,1,\dots,p-1$, then the corresponding lower faces become $-q^{-1}, -q^{-1}+1, -q^{-1}+2, \dots, -q^{-1}+p-1$ (reduced mod p). Because $-q^{-1}$ has an inverse in $\mathbb{Z}_p$, notably $-q$, $\{0, -q^{-1}, 2(-q^{-1}), \dots, (p-1)(-q^{-1})\} = \{0,1,2,\dots,p-1\}$, and identifying the wedge-faces according to the given labelling (FIG 28) gives a complete circuit, resulting in a solid toroidal form with a "flat" and a "ridged" side (FIG 29).

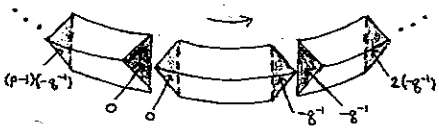

FIG 28

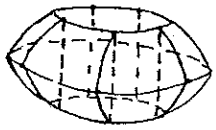

FIG 29

The p dotted lines shown in FIG 29 are equally spaced around the cylindrical hole through the ridged solid torus and correspond to the p pairs of corresponding arcs along the rims of the wedge faces in FIG 27. Hence, if joined end-to-end in their original order $(0,1,2,\dots,p-1)$ = $(0(-q^{-1}), -q(-q^{-1}), -2q(-q^{-1}), \dots, -(p-1)q(-q^{-1}))$ (all reduced mod p), they form a copy of the meridian m.

Now in FIG 28, the dotted lines lie sequentially as the multiples of $(-q^{-1})$, so a joining order for the vertical segments of FIG 24 corresponding, under translation, to the above joining order for the cylindrical hole of FIG 29 is simply $(0, -q, -2q, \dots, -(p-1)q)$ (all reduced mod p). This is the order in which the segments of FIG 24 were originally joined in the torus knot (p,q); to see this, apply a $\frac{2\pi(-q)}{p}$-radian twist to the solid cylinder and orthogonally identify the ends, to return to T_2.

So by inserting this cylinder-with-twist-identified-ends into the hole of FIG 29 in such a way that the vertical segments coincide, we are effectively reversing the Heegaard splitting which gave rise to our initially-described Heegaard diagram. It follows that $L(p,q)$, as defined in model 1.3, is homeomorphic to a lens-shaped solid with various regions of the upper and lower caps identified.

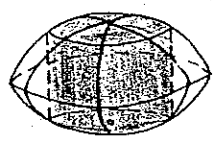

FIG 30

The upper and lower faces of the cylindrical core are identified after a $\frac{2\pi q}{p}$-radian twist. Further, the upper and lower "panels" of the ridged solid torus of FIG 29 are identified after the same $\frac{2\pi q}{p}$ twist. To see this, label the panels of each wedge as shown in FIG 31.

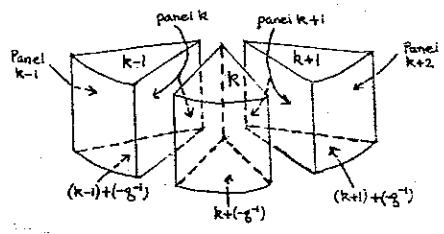

FIG 31

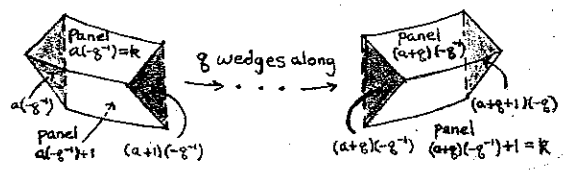

FIG 32

Because $a(-q^{-1}) = (a+q)(-q^{-1})+1$, the upper panel of a wedge is identified with the lower panel of the q-th wedge along from it, traversing the ring in the positive direction (refer to FIG 32). This accounts for the $\frac{2\pi q}{p}$-radian twist. So the $L(p,q)$ of model 1.3 is homeomorphic to the lensform with the identifications described in model 1.2. This proves the equivalence of models 1.2 and 1.3.

This equivalence is demonstrated in [19] and [24] among others, but in the reverse direction. That is, a core is removed from the lensform representation, and the two pieces are reidentified to give two solid tori and a Heegaard identification between their surfaces. The advantage of the "constructive" demonstration included above lies in the explicit determination of the wedge-joining order, which can be (and invariably is) overlooked in the reverse demonstrations.

1.4 A fourth model of $L(p,q)$ can be defined as follows: $L(p,q)$ is the 3-manifold resulting from a p/q Dehn surgery performed along the trivial knot. Once this definition has been explained, it will be fairly easy to see that it describes the space $L(p,q)$ of 1.3.

1.4.1 The concept of surgery was first introduced by Dehn in his 1910 construction of the Poincaré Homology Sphere. It is a method of constructing 3-manifolds by removing finitely many mutually disjoint solid tori from S^3 and then "sewing them back differently". More precisely, select and remove n mutually disjoint solid tori $T_1,\dots,T_n$ (possibly knotted or linked) from S^3 and take the closure $\overline{S^3-(T_1\cup\cdots\cup T_n)}$. Now suppose there is a homeomorphism $h:\partial T_1\cup\cdots\cup\partial T_n \to \partial T_1\cup\cdots\cup\partial T_n$ such that each $h|\partial T_i$ is a homeomorphism $h_i:\partial T_i\to\partial T_i$ $(1\le i\le n)$. Then h implicitly describes how the $T_1,\dots,T_m$ are to be resewn into $\overline{S^3-(T_1\cup\cdots\cup T_n)}$: simply reidentify the boundaries of the T_i via the h_i. The resulting 3-manifold $M=\overline{S^3-(T_1\cup\cdots\cup T_n)}\cup_h(T_1\cup\cdots\cup T_n)$ is then said to have been obtained from Dehn surgery on S^3.

1.4.2 M is entirely determined by $T_1,\dots,T_n$ and h, so surgery instructions are introduced to present this information in a concise and useful format. These appear primarily in [19], but equivalent notations also appear in [16] and [24], among others. The T_i can be described by a link L, with components $L_1,\dots,L_n$ of which $T_1,\dots T_n$ are disjoint tubular neighbourhoods, respectively. The homeomorphism h can be described by a collection of integer pairs $(a_1,b_1),\dots,(a_n,b_n)$. This is accomplished by fixing a canonical latitude, meridian pair ℓ_i, m_i on each ∂T_i (orientations related as in FIG 33) so that $h_i(m_i)$ is homotopic to $a\ell_i+bm_i$ for some $a_i,b_i\in\mathbb{Z}$ with $\gcd(a_i,b_i)=1$. It follows from results in [19] that once L and the corresponding (a_i,b_i) are given, any choice of

(i) mutually disjoint tubular neighbourhoods T_i of the L_i

(ii) properly-oriented latitude, meridian pairs ℓ_i, m_i on the respective ∂T_i

(iii) homeomorphism h such that each $(h|\partial T_i)(m_i)$ is equivalent to $a_i\ell_i+b_im_i$ $(1\le i\le n)$

will yield a manifold homeomorphic to M.

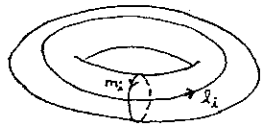

If we sink ℓ_i slightly below the surface of the torus, m_i will have a right-handed orientation with respect to it.

FIG 33

So M is described up to homeomorphism by a link L and a collection $\{(a_1,b_1),\dots,(a_n,b_n)\}$. There is a minor ambiguity, in that each ℓ_i, m_i pair has two possible orientations, so (a_i,b_i) is interchangeable with $(-a_i,-b_i)$. This can be eliminated by considering the rationals b_i/a_i. We permit $\pm 1/0$ and denote it by ∞. Hence our surgery instructions for the construction of a 3-manifold M have been reduced to a link and a rational number (or ∞) assigned to each component thereof.

1.4.3 S^3 can be decomposed into two solid tori such that a meridian on one is identified with a latitude on the other, and vice-versa. This is demonstrated by the cross-section diagrams of FIG 34.

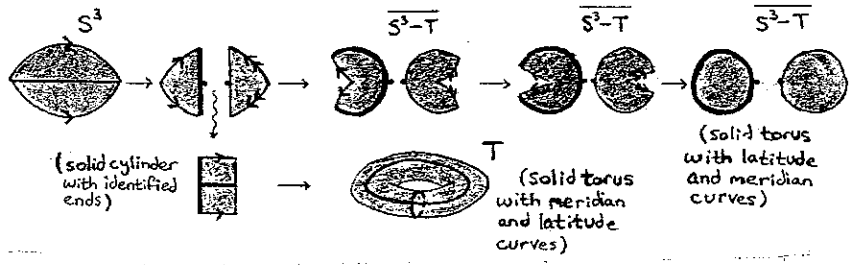

FIG 34

1.4.4 We will now proceed to follow the surgery instructions given for $L(p,q)$ at the beginning of this section. First remove a tubular neighbourhood of the trivial knot from S^3. This will be an unknotted solid torus T, and when the closure $\overline{S^3-T}$ is taken, the result is a second solid torus. Next, T must be resewn to $\overline{S^3-T}$ via some homeomorphism $h: \partial T \to \partial T$ with $h(m) = q\ell + pm$, where ℓ, m is a properly-oriented latitude, meridian pair. Using an alternate notation, $h((0,1)) = (q,p)$. Since latitudes and meridians are interchanged between T and S^3-T, a (q,p) knot on the toroidal hole left by T is in fact a (p,q) knot on the solid torus $\overline{S^3-T}$. Therefore, the manifold obtained from this surgery is the result of sewing two solid tori together via a surface identification which takes a meridian $(0,1)$ to a torus knot (p,q). The identification via h is therefore a reversal of the Heegaard splitting for $L(p,q)$ as described by model 1.3. So we see that $L(p,q)$ as described by the surgery instructions in 1.4 is equivalent to $L(p,q)$ as described by the three previous models.

1.4.5 It is interesting to note that a theoretical result in [12] states that any finite orientable 3-manifold M which can be represented by a Heegaard diagram can be obtained from a Dehn surgery. [24] includes a proof of this by induction on the Heegaard genus M which introduces "twisting" homeomorphisms for methodically manipulating curves on handlebody surfaces. These appear, albeit in a limited capacity, in the next model of $L(p,q)$.

~

1.5 The fifth and final model of $L(p,q)$ is based on the concept of the branched cover, and is described as follows : $L(p,q)$ is the 2-sheeted cover of S^3 branched over the closed rational tangle p/q. This result is mentioned in varying guises and with varying amounts of justification, in [6], [7], [15], [19], and [21]. The most rigorous outline, perhaps, is to be found in [6], although the approach is an almost entirely knot theoretical one.

The appropriate terminology will be introduced, and then this model will be shown to be equivalent to 1.3. It is a rather involved model, but serves to illustrate an important relationship between lens spaces and knot theory, and introduces a useful matrix notation which is to be applied in section 2.

1.5.1 Let $M, \tilde{M}$ be n-manifolds (or n-manifolds-with-boundaries) and $\tilde{L} \subseteq \tilde{M}$, $L \subseteq M$ be $(n-2)$-manifolds (or $(n-2)$-manifolds-with-boundaries).
If there exists some continuous surjective $p: \tilde{M} \to M$ such that
(i) $p(\tilde{L}) = L$
(ii) $p|\tilde{M}\setminus\tilde{L} : \tilde{M}\setminus\tilde{L} \to M\setminus L$ is a k-fold covering map. That is, each point in $M\setminus L$ has an open neighbourhood $\mathcal{U}$ such that $(p|\tilde{M}\setminus\tilde{L})^{-1}(\mathcal{U})$ consists of k disjoint components, each of which $p|\tilde{M}\setminus\tilde{L}$ maps homeomorphically onto $\mathcal{U}$.
(iii) $|p^{-1}(\{x\})| = k$ if $x \in M\setminus L$ and $|p^{-1}(\{x\})| < k$ if $x \in L$ (the first condition follows from (ii))
then $\tilde{M}$ is said to be a <u>k-sheeted cover of M branched over L</u>. L is called the <u>branching locus</u>.

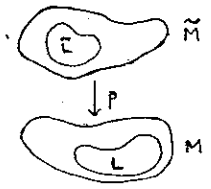

FIG 35

1.5.2 The annulus A is a 2-sheeted cover of the disc D branched over two distinct interior points (FIG 36).

FIG 36

FIG 37

To see this, disconnect A along the dotted circle shown in FIG 37. Note that A and D are 2-manifolds-with-boundaries, and the branching locus is a 0-manifold.

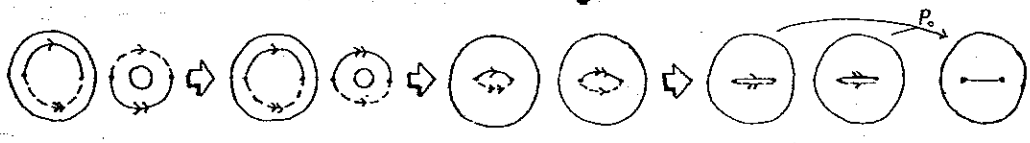

FIG 38

p_0 shown in FIG 38 translates points from the two perforated discs onto their corresponding points in D. As required, all points in D have 2-point preimages in A, except the branch points, which have 1-point preimages. To ensure that $p_0 : A\setminus\{\text{branch pts.}\} \to D\setminus\{\text{branch pts.}\}$ would be a 2-fold covering map, the "inner half" of A was "turned over" on removal (second step, FIG 38). Given points of D not lying on the segment joining the branch points, we can choose circular neighbourhoods sufficiently small so as not to intersect the segment, and these have the required p_0-preimages. Small circular neighbourhoods of points lying on the segment also have the required preimages, since the upper and lower halves of the preimage components are reidentified correctly (this is why the inner half of A must be turned over.). Boundary points are treated similarly.

1.5.3 A solid torus T can be viewed as $A \times I$, and a 3-ball B (homeomorphic to D^3) as $D \times I$. If we define a map $p_t : A \times \{t\} \to D \times \{t\}$ for each $t \in [0,1]$, analagous to the already-defined mapping p_0, and denote the collective mapping $p : T \to B$, then we see that p provides a 2-sheeted cover of B by T which is branched over two disjoint, unlinked arcs. (That 1.5.1 (i) and (iii) hold is immediately obvious, and to verify (ii), simply choose $\mathcal{U} \times I$ where $\mathcal{U}$ is chosen on a given $D \times \{t_0\}$ as before)

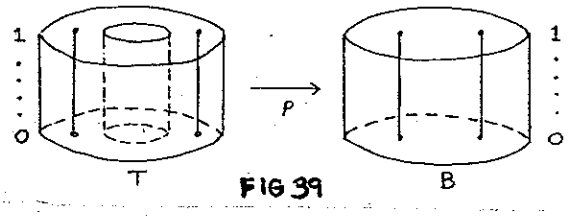

FIG 39

By considering FIG 41, we see that in FIG 40, the p-preimage of the shaded region on ∂B is the shaded region on ∂T.

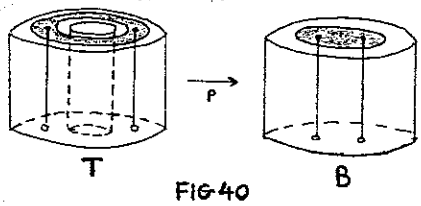

FIG 40

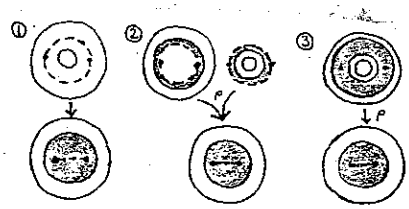

FIG 41

By considering FIG 43, we see that in FIG 42, the p-preimage of the shaded region on ∂B is homeomorphic to the shaded region shown on ∂T.

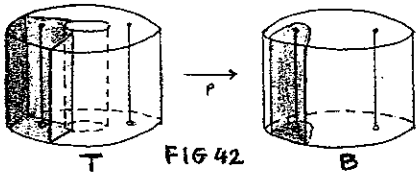

FIG 42

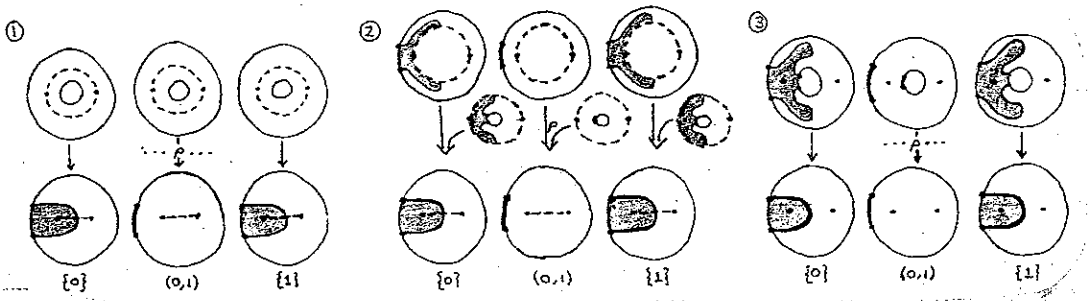

FIG 43

Now referring back to FIG 40, a "half-twist" on the shaded disc corresponds, under p, to a "full-twist" on the shaded annulus (FIG 44).

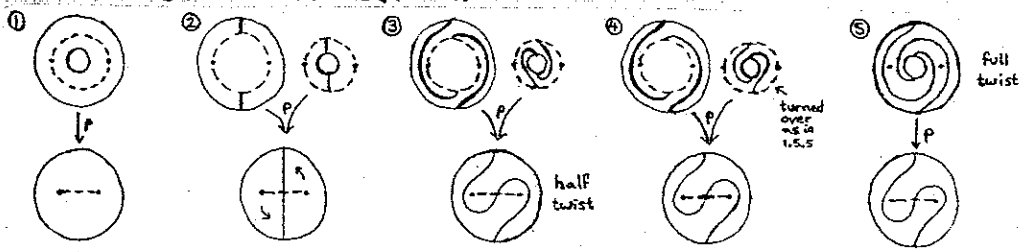

FIG 44

Referring to FIG 42, the shaded region on ∂T is homeomorphic to an annulus and the region on ∂B to a disc, p mapping the former onto the latter as a 2-sheeted cover branched over the two endpoints of the arc. We can devise a similar sequence of steps to the one shown in FIG 44 (although significantly longer and more tedious) to demonstrate that a half twist on the disc corresponds to a full twist on the annulus.

1.5.4 We now define homeomorphisms $h_1, h_2 : \partial B \to \partial B$ and $\tilde{h}_1, \tilde{h}_2 : \partial T \to \partial T$.
h_1 is the identity for points outside the shaded disc of FIG 40 and acts on the disc as suggested in FIG 45. h_2 is the identity for points outside the shaded region of FIG 42 and acts on the region as suggested in FIG 46.

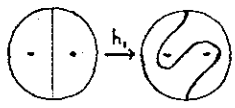

FIG 45

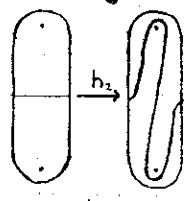

FIG 46

$\tilde{h}_1$ is the identity for points outside the shaded annulus of FIG 40 and performs a positive full-twist on the annulus itself. $\tilde{h}_2$ is the identity for points outside the shaded annulus of FIG 42 and performs a negative full twist on the annulus itself.

If we consider two copies of T and two of B, denoted T_1, T_2 and B_1, B_2, then by remarks in 1.5.3, the following diagram commutes:

$$\begin{tikzcd} \partial T_1 \arrow[r, "\tilde{h}_1"] \arrow[d, "p"'] & \partial T_2 \arrow[d, "p"] \\ \partial B_1 \arrow[r, "h_1"'] & \partial B_2 \end{tikzcd} \qquad \begin{tikzcd} \partial T_1 \arrow[r, "\tilde{h}_2"] \arrow[d, "p"'] & \partial T_2 \arrow[d, "p"] \\ \partial B_1 \arrow[r, "h_2"'] & \partial B_2 \end{tikzcd}$$

FIG 47

So $h_1 p = p\tilde{h}_1$ and $h_2 p = p\tilde{h}_2$. In this case, we will say h_1, h_2 <u>lift</u> to $\tilde{h}_1, \tilde{h}_2$ (with respect to p), respectively.

1.5.5 If $h : \partial B_1 \to \partial B_2$ is a homeomorphism, then we can sew two copies of B together by identifying boundaries via h. The resulting space will be denoted $B_1 \underset{h}{\cup} B_2$. Sewing B to B via the identity i gives S^3, as shown (in reverse order) in FIG 48.

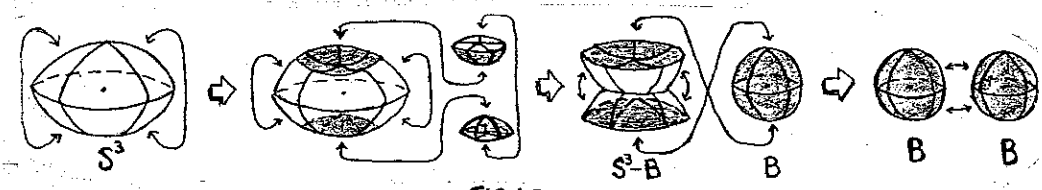

FIG 48

1.5.6 Any composition h of h_1's and h_2's leaves all points of ∂B fixed, except those in a particular region homeomorphic to an open disc (FIG 49). As a result, we can quite easily construct a homeomorphism between $B_1 \underset{h}{\cup} B_2$ and $B_1 \underset{i}{\cup} B_2 \cong S^3$ (FIG 50).

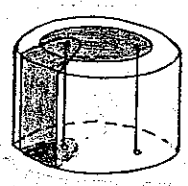

FIG 49

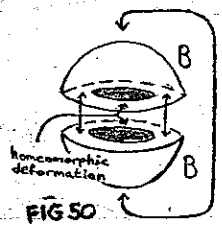

FIG 50

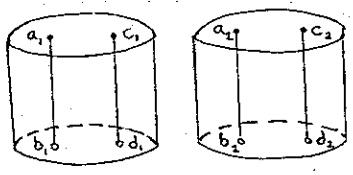

B_1 FIG 51 B_2

1.5.7 For reasons which will become obvious, we will only consider the sewing together of B's via maps which permute the four branch points lying on ∂B. Using the labelling of FIG 51, here are some examples of acceptable joinings:

Sewing B_1 to B_2 via i gives the permutation $(a_1 b_1 c_1 d_1) \to (a_2 b_2 c_2 d_2)$
Sewing B_1 to B_2 via h_1 gives the permutation $(a_1 b_1 c_1 d_1) \to (c_2 b_2 a_2 d_2)$
Sewing B_1 to B_2 via h_2 gives the permutation $(a_1 b_1 c_1 d_1) \to (b_2 a_2 c_2 d_2)$

The results of these identifications will be copies of S^3 containing various links corresponding to the branching loci, as in FIG 52.

FIG 52

The link corresponding to a composition of h_1's and h_2's can be constructed by simply adding the appropriate crossings in the correct order. FIG 53 gives some examples.

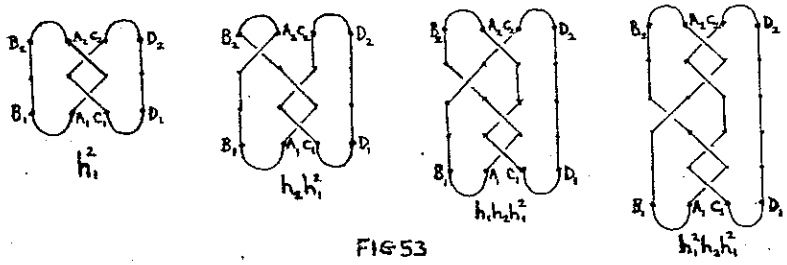

FIG 53

Note 1: The differing crossing orders for h_1 and h_2 result from the differing orientations of the twists.
Note 2: Crossings are added from bottom to top in FIG 53 because h identifies $x \in \partial B_1$ with $h(x) \in \partial B_2$

1.5.8 <u>Lemma</u>: Suppose, for $i=1,2$, p_i provides a 2-sheeted cover of T_i over B_i branched along L_i (where L_i and $\tilde{L}_i = p_i^{-1}(L_i)$ are the pairs of disjoint arcs suggested in FIG 54). Let $h: \partial B_1 \to \partial B_2$ permute the set of surface branch points (i.e. $\{h(a_1), h(b_1), h(c_1), h(d_1)\} = \{a_2, b_2, c_2, d_2\}$) and lift to $\tilde{h}: \partial T_1 \to \partial T_2$ (i.e. $hp_1 = p_2\tilde{h} : \partial T_1 \to \partial B_2$). Then $T_1 \cup_{\tilde{h}} T_2$ is a 2-sheeted cover of $B_1 \cup_h B_2$ branched over $L_1 \cup_h L_2$.

<u>Proof</u>: We define $P: T_1 \cup_{\tilde{h}} T_2 \to B_1 \cup_h B_2$ by $P(x) = \begin{cases} p_1(x) & \text{if } x \in T_1 \\ p_2(x) & \text{if } x \in T_2 \end{cases}$. It must be confirmed that P is consistent at the boundaries ∂T_i. Suppose $x_1 \in \partial T_1$ and $x_2 \in \partial T_2$ are identified: $x_2 = \tilde{h}(x_1) \Rightarrow p_2(x_2) = p_2(\tilde{h}(x_1)) = p_2\tilde{h}(x_1) = hp_1(x_1)$ (by lifting properties). $P(x_1) = p_1(x_1) \in \partial B_1$ and $P(x_2) = p_2(x_2) \in \partial B_2$ are identified, so P takes identified points to identified points, and is therefore consistent.
1.5.1 (i) is satisfied, since $P(\tilde{L}_1 \cup_{\tilde{h}} \tilde{L}_2) = P(\tilde{L}_1) \cup_h P(\tilde{L}_2) = p_1(\tilde{L}_1) \cup_h p_2(\tilde{L}_2) = L_1 \cup_h L_2$.
1.5.1 (ii) and (iii) are satisfied for points in the $\mathring{B}_i$, since $P: \mathring{T}_i \to \mathring{B}_i$ acts as $p_i: \mathring{T}_i \to \mathring{B}_i$ providing the existence of the required open neighbourhoods and correct preimage-set cardinalities.
We must now check the validity of 1.5.1 (ii) and (iii) on the ∂B_i:
$x \in \partial B_1$ is a branch point $\Leftrightarrow h(x) \in \partial B_2$ is a branch point, because h permutes the branch points, so $|P^{-1}(\{x\})| = |p_1^{-1}(\{x\})| = |p_2^{-1}\{h(x)\}| = \begin{cases} 1 & \text{if } x \text{ is a branch point} \\ 2 & \text{if } x \text{ is not a branch point} \end{cases}$, satisfying (iii).
Constructing the required open neighbourhood of $x \sim h(x)$ in $B_1 \cup_h B_2$ to satisfy (ii) is a particularly involved process, which I shall outline here: First we select S_1, S_2 which are open neighbourhoods of $x, h(x)$ in B_1, B_2 respectively, and which satisfy condition (ii) for the mappings $p_i: T_i \to B_i$, $i=1,2$, respectively. Although $S_1 \cap \partial B_1$ and $S_2 \cap \partial B_2$ may not "match up" under h, it isn't difficult to choose open neighbourhoods of $x, h(x)$ contained in the S_i, say $W_1 \subseteq S_1$ and $W_2 \subseteq S_2$, where $W_1 \cap \partial B_1$ and $W_2 \cap \partial B_2$ <u>do</u> match up under h, so that $W_1 \cup_h W_2$ is well-defined. By properties of the p_i already established, the W_i will have the correct p_i-preimages. That is, each $p_i^{-1}(W_i)$ will have two components, U_i and V_i, each of which is mapped homeomorphically onto the W_i by the appropriate restriction of p_i. Since $\tilde{h}(p_1^{-1}(U_1) \cap \partial T_1) = (p_2^{-1}(W_2) \cap \partial T_2)$ (this can be shown

with two set-inclusion arguments, making use of the lifting properties of h) and $U_i \cap V_i = \phi$, the sets $U_1 \cap \partial T_1$, $V_1 \cap \partial T_1$ match up with $U_2 \cap \partial T_2$, $V_2 \cap \partial T_2$ under $\tilde{h}$, although not necessarily in the desired order. However, by renaming U_2, V_2 if necessary, we can assume wlog that $\tilde{h}(U_1 \cap \partial T_1) = U_2 \cap \partial T_2$ and $\tilde{h}(V_1 \cap \partial T_1) = V_2 \cap \partial T_2$. So $U_1 \underset{h}{\cup} U_2$ and $V_1 \underset{h}{\cup} V_2$ are two well-defined open sets in $T_1 \underset{h}{\cup} T_2$, disjoint, with

$$\left.\begin{aligned} [P|(U_1 \underset{h}{\cup} U_2)](U_1 \underset{h}{\cup} U_2) &= (p_1|U_1)(U_1) \underset{h}{\cup} (p_2|U_2)(U_2) = W_1 \underset{h}{\cup} W_2 \\ [P|(V_1 \cup V_2)](V_1 \underset{h}{\cup} V_2) &= (p_1|V_1)(V_1) \underset{h}{\cup} (p_2|V_2)(V_2) = W_1 \underset{h}{\cup} W_2 \end{aligned}\right\} \text{(homeomorphic mappings)}$$

$P^{-1}(W_1 \underset{h}{\cup} W_2) = p_1^{-1}(W_1) \underset{h}{\cup} p_2^{-1}(W_2) = (U_1 \underset{h}{\cup} U_2) \cup (V_1 \underset{h}{\cup} V_2)$, so $W_1 \underset{h}{\cup} W_2$ has the correct P preimage, and is the required neighbourhood of $x \sim h(x)$ in $B_1 \underset{h}{\cup} B_2$ to satisfy (ii).

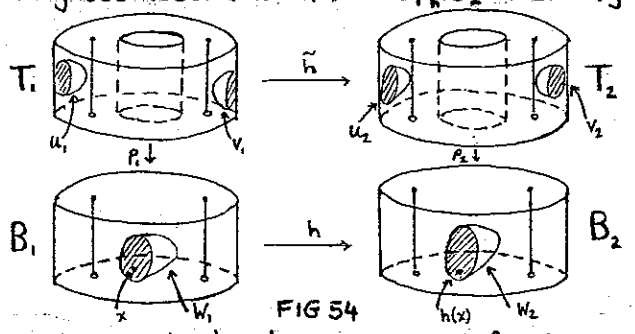

FIG 54

1.5.9 The Dehn twist about a simple closed curve c (with fixed orientation) on ∂T is a homeomorphism $\partial T \to \partial T$ which results from the following procedure: Disconnect an annular neighbourhood of c (sufficiently narrow not to be self-intersecting - as in FIG 55), perform a full twist of one edge with respect to the other (as in FIG 56), then rejoin.

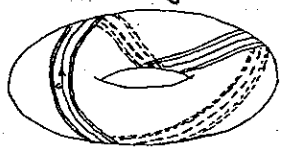

FIG 55

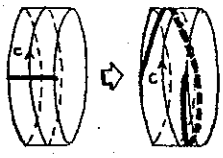

FIG 56

A Dehn twist about a meridian m is a meridianal Dehn twist (denoted $M: \partial T \to \partial T$), and one about a latitude is a latitudinal Dehn twist (denoted $L: \partial T \to \partial T$). $\tilde{h}_1$, $\tilde{h}_2$ as defined in 1.5.4 can now be seen to be equivalent to L, M respectively.

1.5.10 As was seen in 1.3, every simple closed curve on a torus is homotopic to a torus knot of the form $a\ell + bm$ (often denoted (a,b)) for some a,b with $\gcd(a,b)=1$, where ℓ is a canonical latitude and m a canonical meridian, with fixed relative orientations as in FIG 33.

1.5.11 Suppose $0<q<p$ with $\gcd(p,q)=1$. We will now examine the effects of L and M on a torus knot $(p,q) \subseteq \partial T$:
L essentially leaves the number of meridianal traversals fixed, but adds it to the number of latitudinal traversals. So $L((p,q)) = (p+q, q) = (p\ q)\begin{pmatrix}1&0\\1&1\end{pmatrix}$, and similarly $M((p,q)) = (p, p+q) = (p\ q)\begin{pmatrix}1&1\\0&1\end{pmatrix}$. Some examples, using the standard torus identification diagram, will serve to illustrate this:

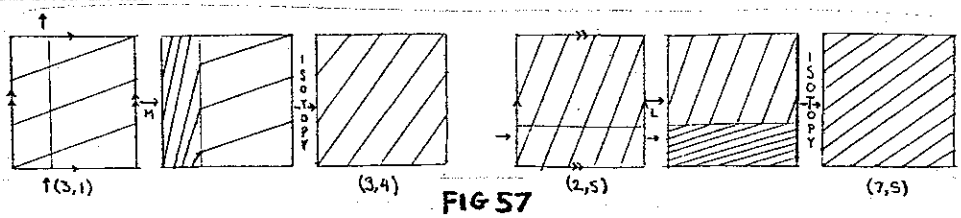

FIG 57

It can easily be shown by induction that $L^k((p,q)) = (p\ q)\begin{pmatrix}1&0\\k&1\end{pmatrix}$, $M^k((p,q)) = (p\ q)\begin{pmatrix}1&k\\0&1\end{pmatrix}$.

1.5.12 Since we have chosen p, q with $0<q<p$ and $\gcd(p,q)=1$, p/q is a positive fraction (in reduced form). Now p/q can always be expressed as a continued fraction, i.e.

$$p/q = d_1 + \cfrac{1}{d_2 + \ddots + \cfrac{1}{d_{n-1} + 1/d_n}}$$

for some n and with each $d_i \in \mathbb{N}$. A procedure for calculating the d_i's is given here: We know $d_1 \leq p/q < d_1+1$ for some $d_1 \in \mathbb{N}$. If $p/q = d_1$, we have a representation. Otherwise, $p/q > d_1 \Rightarrow 0 < p/q - d_1 < 1 \Rightarrow \frac{1}{p/q - d_1} > 1 \Rightarrow d_2 \leq \frac{1}{p/q - d_1} < d_2+1$ for some $d_2 \in \mathbb{N}$. If $d_2 = \frac{1}{p/q - d_1}$ then $p/q = d_1 + 1/d_2$, and we have a representation. Otherwise, $\frac{1}{p/q - d_1} > d_2 \Rightarrow 0 < \frac{1}{p/q - d_1} - d_2 < 1$ $\Rightarrow \frac{1}{\frac{1}{p/q - d_1} - d_2} > 1 \Rightarrow d_3 \leq \frac{1}{\frac{1}{p/q - d_1} - d_2} < d_3+1$ for some $d_3 \in \mathbb{N}$, and we can continue to generate the d_i's in this way. That the sequence will terminate is not immediately apparent; however, on careful examination this can be seen to be the case. An example may shed some light on this:

$$\frac{273}{118} = 2 + \frac{1}{118/37} = 2 + \cfrac{1}{3 + \cfrac{1}{37/7}} = 2 + \cfrac{1}{3 + \cfrac{1}{5 + \cfrac{1}{7/2}}} = 2 + \cfrac{1}{3 + \cfrac{1}{5 + \cfrac{1}{3 + \cfrac{1}{2/1}}}}$$

Observe the numerator/denominator pattern in the sequence $\frac{273}{118}, \frac{118}{37}, \frac{37}{7}, \frac{7}{2}, \frac{2}{1}$.
It can be assumed wlog that n is odd, since if n is even:

$$d_n > 1 \Rightarrow p/q = d_1 + \cfrac{1}{d_2 + \cdots + \cfrac{1}{d_{n-1} + \cfrac{1}{(d_n - 1) + (1/1)}}}$$

$$d_n = 1 \Rightarrow p/q = d_1 + \cfrac{1}{d_2 + \cdots + \cfrac{1}{d_{n-1} + \cfrac{1}{(d_{n-1}+1)}}}$$

both of these have an odd number of terms

So we can always obtain a canonical representation for p/q with an odd number of terms. Some examples:

$\frac{41}{18} = 2 + \cfrac{1}{3 + \cfrac{1}{1 + \cfrac{1}{1 + 1/2}}}$: $d_1 = 2, d_2 = 3, d_3 = 1, d_4 = 1, d_5 = 2$ (n is odd - this is acceptable)

$\frac{55}{42} = 1 + \cfrac{1}{3 + \cfrac{1}{4 + 1/3}}$: $d_1 = 1, d_2 = 3, d_3 = 4, d_4 = 3$ n is even, so we reassign: $d_1 = 1, d_2 = 3, d_3 = 4, d_4 = 2, d_5 = 1$. This gives

$\frac{55}{42} = 1 + \cfrac{1}{3 + \cfrac{1}{4 + \cfrac{1}{2 + 1/1}}}$ as required.

1.5.13 Suppose $\alpha/\beta = e_1 + \cfrac{1}{e_2 + \cdots + 1/e_n}$ where n is odd, and each $e_i \in \mathbb{N}$. Then the closed rational tangle α/β, sometimes denoted  , is the link described by FIG 58. According to [21], this is a knot when p is odd. It is sometimes called a rational link or rational knot (depending on the number of components). Knot theorists will also recognise it as an example of a 2-bridge knot and a 4-braid (Viergenflechte).

The example for $9/7 = 1 + \cfrac{1}{3 + \cfrac{1}{2}}$ is shown in FIG 59.

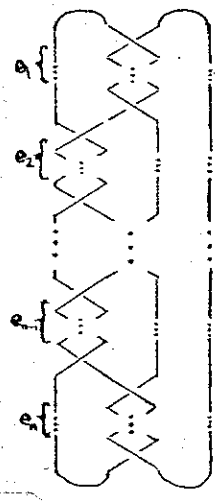

FIG 58

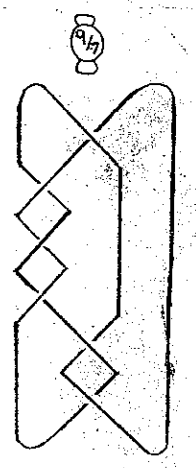

FIG 59

1.5.14 <u>Lemma</u>: If $\begin{bmatrix}1&0\\c_1&1\end{bmatrix}\begin{bmatrix}1&c_2\\0&1\end{bmatrix}\begin{bmatrix}1&0\\c_3&1\end{bmatrix}\cdots\begin{bmatrix}1&0\\c_{n-2}&1\end{bmatrix}\begin{bmatrix}1&c_{n-1}\\0&1\end{bmatrix}\begin{bmatrix}1&0\\c_n&1\end{bmatrix}=\begin{bmatrix}\alpha&\beta\\\gamma&\delta\end{bmatrix}$ where each $c_i\in\mathbb{N}$, then

$$\gamma/\delta = c_n + \cfrac{1}{c_{n-1}+\ddots+\cfrac{1}{c_2+1/c_1}}.$$ Note that n must be odd.

<u>Proof</u>: (By induction) If $n=1$, $\begin{bmatrix}1&0\\c_1&1\end{bmatrix}$ has $c_1/1=c_1$ as required. Now assume the result holds for n. We will show that it holds for $n+2$.

$\begin{bmatrix}1&0\\c_1&1\end{bmatrix}\begin{bmatrix}1&c_2\\0&1\end{bmatrix}\cdots\begin{bmatrix}1&c_{n-1}\\0&1\end{bmatrix}\begin{bmatrix}1&0\\c_n&1\end{bmatrix}=\begin{bmatrix}\alpha&\beta\\\gamma&\delta\end{bmatrix}\Rightarrow$

$\begin{bmatrix}1&0\\c_1&1\end{bmatrix}\begin{bmatrix}1&c_2\\0&1\end{bmatrix}\cdots\begin{bmatrix}1&c_{n-1}\\0&1\end{bmatrix}\begin{bmatrix}1&0\\c_n&1\end{bmatrix}\begin{bmatrix}1&c_{n+1}\\0&1\end{bmatrix}\begin{bmatrix}1&0\\c_{n+2}&1\end{bmatrix}=\begin{bmatrix}\alpha&\beta\\\gamma&\delta\end{bmatrix}\begin{bmatrix}1+c_{n+1}c_{n+2}&c_{n+1}\\c_{n+2}&1\end{bmatrix}=\begin{bmatrix}\alpha+\alpha c_{n+1}c_{n+2}+\beta c_{n+2}&\alpha c_{n+1}+\beta\\\gamma+\gamma c_{n+1}c_{n+2}+\delta c_{n+2}&\gamma c_{n+1}+\delta\end{bmatrix}$

and $\dfrac{\gamma+\gamma c_{n+1}c_{n+2}+\delta c_{n+2}}{\gamma c_{n+1}+\delta} = c_{n+2}+\dfrac{\gamma}{\gamma c_{n+1}+\delta} = c_{n+2}+\dfrac{1}{c_{n+1}+\frac{1}{(\gamma/\delta)}} = c_{n+2}+\cfrac{1}{c_{n+1}+\cfrac{1}{c_n+\ddots+\cfrac{1}{c_2+(1/c_1)}}}$

(by induction hypothesis) as required. So the result holds for $n+2$ and hence for all $n\geq 1$.

1.5.15 <u>Lemma</u>: $\tilde{h}_1^{c_n}\tilde{h}_2^{c_{n-1}}\cdots\tilde{h}_2^{c_2}\tilde{h}_1^{c_1}:\partial T\to\partial T$ is a lift of $h_1^{c_n}h_2^{c_{n-1}}\cdots h_2^{c_2}h_1^{c_1}:\partial B\to\partial B$ with respect to p.

<u>Proof</u>: $p(\tilde{h}_1^{c_n}\tilde{h}_2^{c_{n-1}}\cdots\tilde{h}_2^{c_2}\tilde{h}_1^{c_1}) = p\tilde{h}_1(\tilde{h}_1^{c_n-1}\tilde{h}_2^{c_{n-1}}\cdots\tilde{h}_2^{c_2}\tilde{h}_1^{c_1}) = h_1p(\tilde{h}_1^{c_n-1}\tilde{h}_2^{c_{n-1}}\cdots\tilde{h}_2^{c_2}\tilde{h}_1^{c_1}) = \cdots$

$\cdots = h_1^{c_n}h_2^{c_{n-1}}\cdots h_2^{c_2}h_1^{c_1-1}p\tilde{h}_1 = (h_1^{c_n}h_2^{c_{n-1}}\cdots h_2^{c_2}h_1^{c_1})p.$

1.5.16 We can now justify the description of $L(p,q)$ given at the outset of 1.5:

If $p/q = c_n+\cfrac{1}{c_{n-1}+\cdots+\cfrac{1}{c_2+1/c_1}}$, then Lemma 1.5.14 gives $(0\,1)\begin{bmatrix}1&0\\c_1&1\end{bmatrix}\begin{bmatrix}1&c_2\\0&1\end{bmatrix}\cdots\begin{bmatrix}1&c_{n-1}\\0&1\end{bmatrix}\begin{bmatrix}1&0\\c_n&1\end{bmatrix}=(\gamma\,\delta)$

where $\gamma/\delta = p/q$. Equivalently, $L^{c_n}M^{c_{n-1}}\cdots M^{c_2}L^{c_1}((0,1)) = (\gamma,\delta)$.

$\begin{vmatrix}\alpha&\beta\\\gamma&\delta\end{vmatrix}=\begin{vmatrix}1&0\\c_1&1\end{vmatrix}\begin{vmatrix}1&c_2\\0&1\end{vmatrix}\cdots\begin{vmatrix}1&c_{n-1}\\0&1\end{vmatrix}\begin{vmatrix}1&0\\c_n&1\end{vmatrix}=1\cdots1=1\Rightarrow\alpha\delta-\beta\gamma=1\Rightarrow\gcd(\gamma,\delta)=1$. And since $\gcd(p,q)=1$, it must be the case that $\gamma=p$ and $\delta=q$, so $\tilde{h}_1^{c_n}\tilde{h}_2^{c_{n-1}}\cdots\tilde{h}_2^{c_2}\tilde{h}_1^{c_1}((0,1))=(p,q)$.

Let $h=h_1^{c_n}h_2^{c_{n-1}}\cdots h_2^{c_2}h_1^{c_1}:\partial B\to\partial B$. Then from Lemma 1.5.15, $\tilde{h}=\tilde{h}_1^{c_n}\tilde{h}_2^{c_{n-1}}\cdots\tilde{h}_2^{c_2}\tilde{h}_1^{c_1}$ is a lift of h (i.e. $p\tilde{h}=hp$). From Theorem 1.5.8, $B_1\cup_h B_2$ has 2-sheeted cover $T_1\cup_{\tilde{h}}T_2$ branched over $L_1\cup_h L_2$. Now $T_1\cup_{\tilde{h}}T_2$ is the 3-manifold resulting from sewing two solid tori together via $\tilde{h}$. We have just seen that $\tilde{h}((0,1))=(p,q)$; that is, $\tilde{h}$ takes a meridian $(0,1)$ on ∂T_1 to a (p,q) torus knot on ∂T_2. Hence, from model 1.3, we see that $T_1\cup_{\tilde{h}}T_2\cong L(p,q)$. Also, recall from 1.5.6, $B_1\cup_h B_2\cong S^3$.

So $L(p,q)$ is the 2-sheeted cover of S^3 branched over $L_1\cup_h L_2$. Using FIGS 52, 53 and 58, we see that $L_1\cup_h L_2$ is the closed rational tangle $c_n+\cfrac{1}{c_{n-1}+\ddots+\cfrac{1}{c_2+1/c_1}}=p/q$.

Hence, as initially proposed, $L(p,q)$ is the 2-sheeted cover of S^3 branched over 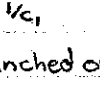 .

1.5.17 The case $L(1,0)$ has not yet been dealt with, as $p/q=1/0$ is not well-defined. However, in 3.2, we will see that $L(1,0)\cong S^3$, and [19] demonstrates that S^3 is a 2-sheeted branched cover of S^3 branched over S^1. This would suggest that in some sense,  is the trivial knot. Carefully adapting the results in this section to allow negative c_i's, it can be seen that $1/0=+\infty=1+\frac{1}{-1+1/1}$ which corresponds to FIG 60, the trivial knot.

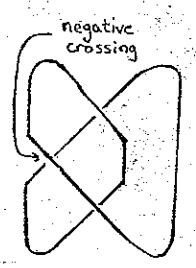

FIG 60

2. MAJOR RESULTS

Some important results concerning 3-dimensional lens spaces, and their proofs where possible, are included here.

2.1 Particular Lens Spaces: Some lens spaces are homeomorphic to more familiar spaces. The violation of our index-convention in the first two examples will be fully explained in 3.2.

2.1.1 Result: $L(0,1) \cong S^1 \times S^2$

Proof: According to model 1.3, $L(0,1)$ is the result of sewing two copies of a solid torus T together via some homeomorphism $h: \partial T \to \partial T$ which takes a meridian to a $(0,1)$ torus knot. This, of course, is just a meridian, so h can be chosen as the identity $i: \partial T \to \partial T$. Now $T = S^1 \times D^2$, and the result of sewing two copies of D^2 together via $i: \partial D^2 \to \partial D^2$ is S^2. Hence, if we sew the solid tori together "one disc at a time", we see that $L(0,1) \cong S^1 \times S^2$.

2.1.2 Result: $L(1,q) \cong S^3 \quad \forall q \in \mathbb{Z}$

Proof: By model 1.2, $L(1,q)$ is the result of orthogonally identifying the upper and lower faces of a lensform after twisting one of the caps $\frac{2\pi q}{1} = 2\pi q$ radians. Since this is equivalent to no twist at all, the result is S^3. (Refer back to 1.2.3)

2.1.3 Result: $L(2,1) \cong \mathbb{R}P^3$

Proof: By model 1.1, $L(2,1) = S^3/\mathbb{Z}_2$. That is S^3, where (z_1, z_2) is identified with (z_1', z_2')

$\Leftrightarrow (z_1', z_2') = (e^{\frac{2\pi i m}{2}} z_1, e^{\frac{2\pi i 1 m}{2}} \cdot z_2)$ for some $m \in \mathbb{Z}_2$

$\Leftrightarrow (z_1', z_2') = (e^{\pi i m} z_1, e^{\pi i m} \cdot z_2)$ for $m = 0$ or 1

$\Leftrightarrow (z_1', z_2') = (z_1, z_2)$ or $-(z_1, z_2)$

So $L(2,1)$ is S^3 with antipodal points identified. This is the definition of real projective space denoted $\mathbb{R}P^3$.

2.2 Fundamental Group: Lens spaces are important examples of spaces with finite fundamental groups. Two separate proofs of the fact that $\pi_1(L(p,q)) \cong \mathbb{Z}_p$ are included here.

2.2.1 Lemma: The continuous image of a path-connected space is path connected.

Proof: If $g: X \to Y$ is continuous and surjective, then given $a, b \in Y$, there exist $a', b' \in X$ with $g(a') = a$, $g(b') = b$ and a path f joining a' to b'. Then gf is a path joining a to b in Y.

2.2.2 Result: $\pi_1(L(p,q)) \cong \mathbb{Z}_p$

Proof (A): The natural projection map $p: S^3 \to S^3/\mathbb{Z}_p \cong L(p,q)$ is continuous, since the open sets of the quotient space $S^3/\mathbb{Z}_p$ are defined in terms of their p-preimages. So $L(p,q)$ is the continuous image of path-connected space S^3, and hence is itself path connected. So $\pi(L(p,q), y_0)$ is effectively independent of y_0. A result in [20] states X is simply-connected $\Rightarrow \pi_1(X/G, y_0) \cong G$, although the proof of this involves fibre coverings, etc. and is beyond the scope of this paper. However, S^3 is known to be simply-connected (see p 131. [11], or p. 96 [1]) so it follows immediately that $\pi_1(L(p,q)) \cong \mathbb{Z}_p$

Proof (B): A more obvious calculation of $\pi_1(L(p,q))$ uses the famous Seifert-Van Kampen Theorem. Using model 1.3, $L(p,q)$ can be represented by two solid tori T_1 and T_2 where ∂T_1 and ∂T_2 are identified in such a way that a $(0,1)$ knot on ∂T_1 becomes a (p,q) knot on ∂T_2. If we define T_1^*, T_2^* to be T_1, T_2 respectively, embedded concentrically within open-frontiered solid tori with slightly larger meridianal radii, then the T_i^* are open, path-connected subsets of $L(p,q)$ with $T_1^* \cap T_2^*$ a thin toroidal shell, also open and path-connected. The standard <u>group presentations</u> are:

$$\left.\begin{array}{l}\pi_1(T_1^*) = \langle a; - \rangle \\ \pi_1(T_2^*) = \langle b; - \rangle\end{array}\right\} \text{ (a solid torus retracts to } S^1 \text{ and has fundamental group } \mathbb{Z})$$

$$\pi_1(T_1^* \cap T_2^*) = \pi_1(\partial T_1) = \langle \ell, m; - \rangle \quad \text{(a torus has fundamental group } \mathbb{Z}^2\text{. See 1.3.8)}$$

If $\psi_1 : T_1^* \cap T_2^* \to T_1^*$ and $\psi_2^* : T_1^* \cap T_2^* \to T_2^*$ denote the natural inclusion maps, then the Seifert Van-Kampen Theorem gives $\pi_1(L(p,q)) = \pi_1(T_1^* \cap T_2^*) = \langle a, b; (\psi_1 \ell)^{-1}(\psi_2 \ell), (\psi_1 m)^{-1}(\psi_2 m) \rangle = \langle a, b; a^{-1}b^r, b^p \rangle$. r is some positive integer, as a latitude ℓ on ∂T_1 becomes some (r,s) knot on ∂T_2, which is simply b^r within T_2^*. The presence of the relation $a^{-1}b^r$ renders a equivalent to b^r, and consequently redundant; a Tieze transformation can be applied to formally remove it. Hence $\pi_1(L(p,q)) = \langle b; b^p \rangle \cong \mathbb{Z}_p$. (For an introduction to retractions, group presentations, Tieze transformations, etc. See [11] or [24].)

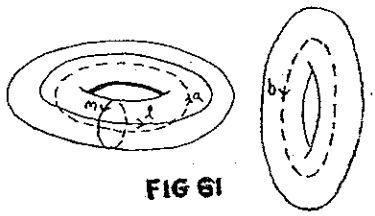

FIG 61

2.3 Homeomorphism Classification:

2.3.1 <u>Lemma</u>: $L(p,q) \cong L(p,-q) \cong L(-p,q) \cong L(-p,-q)$. Obviously, some of these representations violate our convention on indices, but we have a valid interpretation if we appeal to model 1.2.

<u>Proof</u>: If we consider the twists of model 1.2, and how they are used to define $L(p,q)$, it becomes clear that $\frac{2\pi(-q)}{(-p)} = \frac{2\pi q}{p}$ and $\frac{2\pi q}{(-p)} = \frac{2\pi(-q)}{p} \Rightarrow L(-p,-q) \cong L(p,q)$ and $L(-p,q) \cong L(p,-q)$. Now consider a lensform L and its mirror image L' reflected across some plane P (FIG 62).

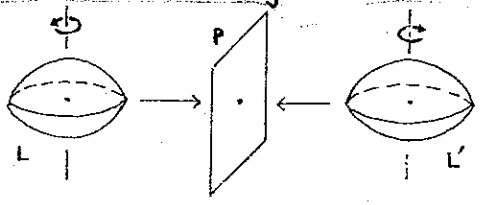

If we perform a set of identifications on L, and the corresponding mirror-image identifications on L', then the resulting identification spaces are clearly homeomorphic. Since a $\frac{2\pi q}{p}$ twist on L corresponds to a $-\frac{2\pi q}{p} = \frac{2\pi(-q)}{p}$ twist on L', it follows immediately that $L(p,q) \cong L(p,-q)$.

2.3.2 <u>Lemma</u>: If $\begin{bmatrix}1&0\\c_1&1\end{bmatrix}\begin{bmatrix}1&c_2\\0&1\end{bmatrix}\cdots\begin{bmatrix}1&c_{n-1}\\0&1\end{bmatrix}\begin{bmatrix}1&0\\c_n&1\end{bmatrix} = \begin{bmatrix}\alpha&\beta\\\gamma&\delta\end{bmatrix}$, then $\begin{bmatrix}1&0\\-c_n&1\end{bmatrix}\begin{bmatrix}1&-c_{n-1}\\0&1\end{bmatrix}\cdots\begin{bmatrix}1&-c_2\\0&1\end{bmatrix}\begin{bmatrix}1&0\\-c_1&1\end{bmatrix} = \begin{bmatrix}\delta&-\beta\\-\gamma&\alpha\end{bmatrix}$ and $\alpha\delta \equiv 1 \pmod{\gamma}$

<u>Proof</u>: Since $\left(\begin{bmatrix}1&0\\c_1&1\end{bmatrix}\cdots\begin{bmatrix}1&0\\c_n&1\end{bmatrix}\right)\left(\begin{bmatrix}1&0\\-c_n&1\end{bmatrix}\cdots\begin{bmatrix}1&0\\-c_1&1\end{bmatrix}\right) = \left(\begin{bmatrix}1&0\\-c_n&1\end{bmatrix}\cdots\begin{bmatrix}1&0\\-c_1&1\end{bmatrix}\right)\left(\begin{bmatrix}1&0\\c_1&1\end{bmatrix}\cdots\begin{bmatrix}1&0\\c_n&1\end{bmatrix}\right) = \begin{bmatrix}1&0\\0&1\end{bmatrix}$ it follows that $\begin{bmatrix}1&0\\-c_n&1\end{bmatrix}\begin{bmatrix}1&-c_{n-1}\\0&1\end{bmatrix}\cdots\begin{bmatrix}1&-c_2\\0&1\end{bmatrix}\begin{bmatrix}1&0\\-c_1&1\end{bmatrix} = \begin{bmatrix}\alpha&\beta\\\gamma&\delta\end{bmatrix}^{-1}$. Because $\begin{vmatrix}\alpha&\beta\\\gamma&\delta\end{vmatrix} = \begin{vmatrix}1&0\\c_1&1\end{vmatrix}\begin{vmatrix}1&c_2\\0&1\end{vmatrix}\cdots\begin{vmatrix}1&c_{n-1}\\0&1\end{vmatrix}\begin{vmatrix}1&0\\c_n&1\end{vmatrix} = 1\cdots 1 = 1$, $\begin{bmatrix}\alpha&\beta\\\gamma&\delta\end{bmatrix}^{-1} = \begin{bmatrix}\delta&-\beta\\-\gamma&\alpha\end{bmatrix}$. And since $\alpha\delta - \beta\gamma = \begin{vmatrix}\alpha&\beta\\\gamma&\delta\end{vmatrix} = 1$, both results follow.

2.3.3 <u>Result</u>: If (1) $q' \equiv \pm q \pmod p$ or (2) $q'q \equiv \pm 1 \pmod p$, then $L(p,q) \cong L(p,q')$

<u>Proof</u>: (1) If $q' \equiv q \pmod p$, then $e^{\frac{2\pi i q'}{p}} = e^{\frac{2\pi i q}{p}}$, so by considering model 1.1, based on group action, we see that $L(p,q) \cong L(p,q')$. Similarly, if $q' \equiv -q \pmod p$, then $L(p,q') \cong L(p,-q) \cong L(p,q)$ by Lemma 2.3.1.

(2) Given $L(p,q)$, we can decompose it into two copies of a solid torus T identified by a homeomorphism $h: \partial T \to \partial T$ such that $h(0,1) = (p,q)$. From an argument in 1.5, h can be chosen as $L^{c_n} M^{c_{n-1}} \cdots M^{c_2} L^{c_1}$, a composition of Dehn twists, where $p/q = c_n + \frac{1}{c_{n-1} + \cdots + \frac{1}{c_1}}$, since this will give the required meridianal image. Now if we switch the rôles of the solid tori, and identify via h^{-1}, the resulting space is still $L(p,q)$. We know $h^{-1}(p,q) = (0,1)$. Let $h^{-1}(0,1) = (p^*, q^*)$, so that $L(p,q) \cong L(p^*, q^*)$. In our case $h^{-1} = L^{-c_1} M^{-c_2} \cdots M^{-c_{n-1}} L^{-c_n}$, so deploying Lemma 2.3.2 and the matrix notation of 1.5 gives $(p\ q) = (0\ 1)\begin{bmatrix} \alpha & \beta \\ \gamma & \delta \end{bmatrix} = (\gamma\ \delta)$ and $(p^*\ q^*) = (0\ 1)\begin{bmatrix} \delta & -\beta \\ -\gamma & \alpha \end{bmatrix} = (-\gamma\ \alpha)$. So $p^* = -p$ and $q^* q \equiv 1 \pmod p$. Hence $L(p,q) \cong L(-p, q^*) \cong L(p, q^*)$ for some q^* with $q^* q \equiv 1 \pmod p$.

Now suppose $qq' \equiv \pm 1 \pmod p$. Then $q(\pm q') \equiv 1 \pmod p \Rightarrow qq^* \equiv q(\pm q') \pmod p \Rightarrow q^* \equiv (\pm q') \pmod p$ (because $\gcd(p,q) = 1$) $\Rightarrow L(p,q^*) \cong L(p,q')$ (by (1)) $\Rightarrow L(p,q) \cong L(p,q')$.

Various proofs of this result can be found in [5], [6], etc., but tend to be more involved. The use of the matrix notation introduced in 1.5 can be put to further use, to simplify such calculations as determining the manifold with surgery instructions $p_1/q_1 \oplus p_2/q_2$ – an otherwise cumbersome task.

The converse of the result, that $L(p,q) \cong L(p,q') \Rightarrow q' \equiv \pm q \pmod p$ or $q'q \equiv \pm 1 \pmod p$ is proved in [5], although the argument is beyond the scope of this paper.

Of course, if $p \neq p'$, $L(p,q) \not\cong L(p',q')$ for all q, q', since the spaces have non-isomorphic fundamental groups.

2.4 <u>Homotopy Classification</u>: Again, note that if $p \neq p'$, then $L(p,q)$ and $L(p',q')$ cannot be homotopy equivalent, since they have non-isomorphic fundamental groups.

2.4.1 <u>Result</u>: $L(p,q)$ is homotopy equivalent to $L(p,q') \Leftrightarrow qq' \equiv \pm m^2 \pmod p$ for some $m \in \mathbb{Z}$.

Necessity is proved in [10] and sufficiency in [27]. The former proof involves block dissections and cohomology theory, while the latter uses incidence matrices. Consequently, both are beyond the scope of this paper.

2.5 <u>Homology Groups</u>:

2.5.1 <u>Result</u>: $H_k(L(p,q)) = \begin{cases} \mathbb{Z} & \text{if } k = 0,3 \\ \mathbb{Z}_p & \text{if } k = 1 \\ 0 & \text{if } k = 2,4,5,6,\ldots \end{cases}$

This can be obtained from results [20] concerning homology and CW-decompositions. An important question that arose in the study of the Poincaré Conjecture was "are two compact connected 3-manifolds with the same homology groups necessarily homeomorphic?" The construction of lens spaces provided an immediate answer of "No" to this question: 2.5.1 states that $L(p,q)$ and $L(p,q')$ have the same homology groups, although we know from 2.3 that they need not be homeomorphic.

3. RELATED SPACES

So far, only the 3-dimensional lensspaces $L(p,q)$ have been investigated. There are several other variations on the same theme which appear scattered throughout the literature. These are briefly described in this section.

3.1 Higher-Dimensional or Generalised Lens Spaces appear in [11], [13], [17], and [23], and can best be seen as an extension of model 1.1. Here $L(p,q)$ was defined as the orbit space of a $\mathbb{Z}_p$-action on S^3. Generalised lens spaces can be constructed for dimensions $0, 5, 7, \ldots, 2n+1, \ldots$ as follows: Let $\mathbb{Z}_p$ act on $S^{2n+1} = \{(z_0,\ldots,z_n) \in \mathbb{C}^{n+1} \mid |z_0|^2+\cdots+|z_n|^2 = 1\}$ so that $m\cdot(z_0,\ldots,z_n) = \left(e^{\frac{2\pi i m}{p}}\cdot z_0,\ e^{\frac{2\pi i m q_1}{p}}\cdot z_1,\ \ldots,\ e^{\frac{2\pi i m q_n}{p}}\cdot z_n\right)$ where each of $q_1,\ldots,q_n$ is chosen to be coprime with p. As in the 3-dimensional case, the action is free, so the orbit space, denoted $L(p,q_1,\ldots,q_n)$ or $L^n(p;q_1,\ldots,q_n)$, is a $2n+1$ manifold with fundamental group $\mathbb{Z}_p$. [23] further defines standard lens spaces to be those of the form $L^n(p;q,\ldots,q)$, whereas [25] defines them to be, more particularly, of the form $L^n(p;1,\ldots,1)$. The latter are referred to as ordinary lens spaces in [13] and denoted $L^n(p)$.

3.2 Degenerate Lens Spaces are 3-dimensional lens spaces with non-standard indices, which can be effectively eliminated from the theory. For example, if $(p,q) = d > 1$, some of the models of $L(p,q)$ in section 1 are meaningless; however, if we appeal to 1.2, we see that by the geometric nature of the group action, the same identifications are taking place as in $L(p/d, q/d)$. The only difference is that a single triangular face in $L(p/d, q/d)$ corresponds to d consecutive faces in $L(p,q)$. So $L(p,q)$ can be regarded as a degenerate lens space. Similarly, if $q \equiv q' \pmod p$, then $e^{\frac{2\pi i q}{p}} = e^{\frac{2\pi i q'}{p}}$ and by model 1.1 $L(p,q) \cong L(p,q')$. So we can restrict q to the range $\{1,\ldots,p-1\}$ to rule out a plethora of degeneracy. Finally, in 2.1 we saw that $L(1,q) \cong S^3$ and $L(0,1) \cong S^1 \times S^2$. [19] remarks that some writers don't consider S^3 and $S^1\times S^2$ to be lens spaces. With reservations, then, we can rule out all $L(p,q)$ with $p=0$ or 1 as degenerate.

N.B. $L(0,1)$ is particularly troublesome, since 1.2 requires a twist of $\frac{2\pi q}{p}$ radians which is not defined in this instance.

3.3 Infinite Lens Spaces make an appearance in [4] as examples of Eilenberg-Maclane spaces. They are denoted $L(\infty,p)$, but best understood as $L^\infty(p)$ (in accordance with the ordinary lens spaces of 3.1). They are obtained as telescopically constructed q-sheeted coverings of S^∞ (the infinite-dimensional sphere). The complete theory behind telescopic construction is beyond the scope of this paper, but the general idea is given here:

$\mathbb{Z}_p$ acts on S^1 to give $L^0(p)$
$\mathbb{Z}_p$ acts on S^3 to give $L^1(p)$
$\vdots$
$\mathbb{Z}_p$ acts on S^{2n+1} to give $L^n(p)$
$\vdots$

There are natural inclusion maps for $S^1 \subseteq S^3 \subseteq \cdots \subseteq S^{2n+1} \subseteq \cdots$. If we glue all of the S^{2n+1} together via these maps and let $\mathbb{Z}_p$ act on the result, the orbit space is $L^\infty(p)$.

4. REFERENCES

1 M.A. ARMSTRONG : Basic Topology , Springer-Verlag , New York (1983)

2 J. BIRMAN : Heegaard splittings of orientable 3-manifolds from Knots, Groups, and 3-Manifolds (ed. L.P. NEUWIRTH) Ann. of Math. Studies no. 84 p 227-259, Princeton University Press (1975)

3 R.L. BISHOP and R.J. CRITTENDEN : Geometry of Manifolds , Academic Press, New York (1964)

4 R. BOTT and L. TU : Differential Forms in Algebraic Topology , Springer-Verlag, New York (1982)

5 E.J. BRODY : The topological classification of the lens spaces , Ann. Math. 71 , p. 163-184 (1960)

6 G. BURDE and H. ZEISCHANG : Knots , de Gruyter, Berlin (1985)

7 J.H. CONWAY : An enumeration of knots and links, and some of their algebraic properties from Computational Problems in Abstract Algebra , Pergamon Press, New York (1970)

8 J. HEMPEL : Construction of orientable 3-manifolds from Topology of 3-Manifolds and Related Topics (ed. M.K. FORT, Jr.) Prentice-Hall (1962)

9 J. HEMPEL : 3-Manifolds , Ann. of Math. Studies no. 86 , Princeton University Press (1976)

10 P.J. HILTON and S. WYLIE : Homology Theory , Cambridge University Press (1960)

11 C. KOSNIOWSKI : A First Course In Algebraic Topology , Cambridge University Press (1980)

12 W.B.R. LICKORISH : A representation of orientable combinatorial 3-manifolds, Ann. Math. 76 , p. 531-540 (1962)

13 N. MAHAMMED, et.al. : Some Applications of Topological K-Theory , North-Holland Math. Studies 45, North-Holland , Amsterdam (1980)

14 C.R.F. MAUNDER : Algebraic Topology , Cambridge University Press (1980)

15 J.M. MONTESINOS : Lectures on 3-fold simple coverings and 3-manifolds from Combinatorial Methods in Topology and Algebraic Geometry (ed. J.R. HARPER and A. MANDELBAUM) Am. Math. Soc. Contemporary Studies vol. 44, p. 157-178 (1985)

16 L. MOSER : Elementary surgery along a torus knot , Pacific J. Math. 38 , p. 737-745 (1971)

17 H. OSBORN : Vector Bundles , Vol. 1 , Academic Press , New York (1982)

18 K. REIDEMEISTER : Homotopieringe und linsenräume , Abh. Math. Sem. Univ. Hamburg 11 , p. 102-109 (1935)

19 D. ROLFSEN : Knots and Links , Publish or Perish, Inc., Berkeley (1976)

20 J. ROTMAN : An Introduction to Algebraic Topology , Springer-Verlag , New York (1988)

21 H. SCHUBERT : Knöten mit zwei brücken , Math Z. 65 , p. 133-170 (1956)

22 H. SEIFERT and W. THRELFALL : A Textbook of Topology, Academic Press , Orlando (1980)

23 D. SJERVE : Geometric dimension of vector bundles over lens spaces , Trans. Am. Math. Soc. 134 p 545-557 (1968)

24 J. STILLWELL : Classical Topology and Combinatorial Group Theory , Springer-Verlag , New York (1980)

25 F. UCHIDA : K-theory of lens-like spaces and S^1 action on $S^{2m+1} \times S^{2n+1}$, Tohoku Math J. 25, p. 201-211 (1975)

26 C.T.C. WALL : Surgery on Compact Manifolds , Academic Press , London (1970)

27 J.H.C. WHITEHEAD : On incidence matrices, nuclei, and homotopy types , Ann. Math. 42 , p 1197-1239 (1941)